Received: 23 September 2022 | Revised: 17 December 2022 | Accepted: 10 January 2023

DOI: 10.1002/mgg3.2140

Molecular Genetics & Genomic Medicine Open Access WILEY

ORIGINAL ARTICLE

Clinical and genetic findings in Chinese families with congenital ectopia lentis

Xin Liu[1] | **Liman Niu**[2] | **Liyun Zhang**[3] | **Liqiong Jiang**[1] | **Kaiqing Liu**[2] | **Xueping Wu**[3] | **Xinhua Liu**[1] | **Jiantao Wang**[1]

[1]Shenzhen Eye Hospital, Jinan University, Shenzhen Eye Institute, Shenzhen, Guangdong, China

[2]Shenzhen Institute of Translational Medicine, The First Affiliated Hospital of Shenzhen University, Shenzhen Second People's Hospital, Shenzhen, Guangdong, China

[3]Postgraduate Training Base of Jinzhou Medical University, Shenzhen Key Laboratory of Ophthalmology, Shenzhen Eye Hospital, Shenzhen, Guangdong, China

Correspondence
Xinhua Liu and Jiantao Wang, Shenzhen Eye Institute, Shenzhen Eye Hospital, Jinan University, 18 Zetian Road, Shenzhen, Guangdong 518040, P.R. China.
Email: xhualiu@sohu.com and wangjiantao65@126.com

Funding information
Shenzhen Excellent Technological and Innovative Talent Training Project, Grant/Award Number: RCBS20200714114818372; National Nature Science Foundation of China, Grant/Award Number: 82070961; Sanming Project of Medicine in Shenzhen, Grant/Award Number: SZSM201812091

Abstract

Background: Congenital ectopia lentis (EL) refers to the congenital dysplasia or weakness of the lens suspensory ligament, resulting in an abnormal position of the crystalline lens, which can appear as isolated EL or as an ocular manifestation of a syndrome, such as the Marfan syndrome. The fibrillin-1 protein encoded by the *FBN1* gene is an essential component of the lens zonules. Mutations in *FBN1* are the leading causes of congenital EL and Marfan syndrome. Owing to the complexity and individual heterogeneity of *FBN1* gene mutations, the correlation between *FBN1* mutation characteristics and various clinical phenotypes remains unclear.

Methods: This study describes the clinical characteristics and identifies possible causative genes in eight families with Marfan syndrome or isolated EL using Sanger and whole-exome sequencing.

Results: Eight *FBN1* mutations were identified in these families, of which three (c.5065G > C, c.1600 T > A, and c.2210G > C) are reported for the first time. Based on in silico analyses, we hypothesized that these mutations may be pathogenic by affecting the fibrillin-1 protein structure and function.

Conclusion: These findings expand the number of known mutations involved in EL and provide a reference for the research on their genotype and phenotype associations.

KEYWORDS
ectopia lentis, *FBN1*, Marfan syndrome, next-generation sequencing

Xin Liu and Liman Niu contributed equally.

1 | INTRODUCTION

Ectopia lentis (EL; Online Mendelian Inheritance in Man (OMIM) 129600) is a displacement of the ocular lens from its normal position due to congenital causes, trauma, or other diseases (Adès et al., 2004). EL may occur independently or as a manifestation of a systemic disorder, such as Marfan syndrome (OMIM 154700), Weill–Marchesani syndrome (OMIM 277600), and homocystinuria (OMIM 236200) (Nelson & Maumenee, 1982). A Danish study showed that the prevalence of congenital EL was approximately 6.4/100,000, of which 68.2% occurred in Marfan syndrome; in comparison, isolated EL and ectopia lentis et pupillae (ELeP) accounted for only 29.2% (Fuchs & Rosenberg, 1998). Marfan syndrome is a hereditary connective tissue disorder characterized by abnormalities in the ocular, cardiovascular, and skeletal systems (Milewicz et al., 2021). Cardiovascular lesions, such as aortic aneurysms and aortic dissections, are the leading causes of death in patients with Marfan syndrome (Milewicz et al., 2021). The revised Ghent criteria the latest international diagnostic criteria for Marfan syndrome, which mainly include family history, aortic root Z-score, EL, systematic score, and *FBN1* mutation (Loeys et al., 2010). Congenital EL is usually a bilateral disease, with an upward or lateral displacement of the lens, typically autosomal dominant, but autosomal recessive inheritance has also been reported (Al-Salem, 1990; Greene et al., 2010). Asymmetric lens dislocation in childhood or adolescence can lead to severe and irreversible amblyopia. As the lens is displaced into the vitreous cavity, leakage of lens protein may occur, leading to chronic vitritis and chorioretinal inflammation (Sadiq & Vanderveen, 2013).

The *FBN1* gene encodes the fibrillin-1 protein and comprises 66 exons on chromosome 15q21.1. Mutation of the *FBN1* gene is the leading cause of congenital EL, with missense mutations being the most common (Chen et al., 2021). Fibrillin-1 is a cysteine-rich glycoprotein that is the major structural component of microfibrils and is ubiquitously found in connective tissues (Sakai & Keene, 2019). Fibrillin-1 comprises 7 transforming growth factor-β1-binding protein-like (TB) domains, 2 hybrid domains, and 47 epidermal growth factor-like (EGF) domains, of which 43have a consensus motif for calcium binding (cb) (Lygia et al., 1993). Approximately 60% of *FBN1* missense mutations occur in the calcium-binding epidermal growth factor (cbEGF)-like domains (Haller et al., 2020). These mutations can affect fibrillin-1 function by replacing the cysteines, preventing the formation of disulfide bonds, or modifying the side chains of the calcium-binding ligands, and thus reducing calcium binding (Zeyer & Reinhardt, 2015). In addition to EL, mutations in *FBN1* can cause segmental zonular damage and global damage, leading to lens defects and microspherophakia, respectively (Hoffman et al., 2013). Furthermore, *FBN1* mutations cause multisystemic connective tissue lesions leading to Marfan syndrome, some of which are accompanied by ocular phenotypes such as EL and retinal detachment (Milewicz et al., 2021). Owing to the heterogeneity of *FBN1* variation, the association between genotype and ocular phenotype and its pathogenesis is currently unclear. With the development of next-generation sequencing (NGS) technology, DNA variation in the genome can be analyzed rapidly and comprehensively on a large scale, which will facilitate the study of the mutational spectrum and provide a reference for the early diagnosis and prevention strategies of EL.

In this study, we recruited eight unrelated Chinese pedigrees in southern China, including six families with isolated EL and two families with Marfan syndrome. Clinical and molecular genetic assessments were conducted to investigate the correlation between the gene mutation type and clinical phenotype. The findings may provide useful insights into the mutation spectrum of congenital EL, facilitating timely treatment of patients.

2 | MATERIALS AND METHODS

2.1 | Patients' data and clinical manifestations

Eight families with congenital EL from Shenzhen Eye Hospital were included in this study. All family members in this study signed an informed consent form and received a comprehensive medical history review, ophthalmologic examination, physical examination, and echocardiography. This study was conducted following the principles of the Declaration of Helsinki and was approved by the Shenzhen Eye Hospital Ethics Committee (no. 2021110402).

2.2 | Whole-exome sequencing

Whole blood samples were collected from 24 individuals for sequencing in this study, including the proband III: 2 and the other family members II: 2 and III: 1 in family 1; the proband II: 1 and the other family members I: 1 and I: 2 in family 2; the proband III: 2 and the other family members II: 1, II: 2, III: 1, and III: 3 in family 3; the proband II: 1 and the other family members I: 1 and I: 2 in family 4; the proband II: 1 and the other family member I: 1 in family 5; the proband II: 1 and the other family member

I: 2 in family 6; the proband III: 1 and the other family members II: 1 and II: 2 in family 7; and the proband II: 1 and the other family members I: 1 and I: 2 in family 8. Approximately 5 ml of whole blood samples were collected from each participant in an EDTA-K2 anticoagulant tube, and genomic DNA was extracted according to the manufacturer's instructions (MagPure Buffy Coat DNA Midi KF Kit, Magen). DNA libraries were constructed by DNA fragmentation, end repair, adapter ligation, and PCR amplification and purification using the MGIEasy DNA Library Prep Kit (MGI). The library was enriched for 12 h at 65°C using array hybridization (KAPA HyperExome, ROCHE). After hybridization, the probe was washed and eluted, and post-PCR purification of the captured samples was performed. After the library was qualified, a single strand of the library products was prepared for circularization, and a DNA nanoball (DNB) was prepared and sequenced using the MGISEQ-2000 platform.

2.3 | Mutation analysis and verification

After sequencing, low-quality reads and adapter sequences were removed, the clean data were aligned with the hg19 genome using Burrows-Wheeler Aligner software, and the single-nucleotide variants (SNVs) and small inversion and deletion (INDEL) were detected using the Genome Analysis Toolkit software. Simultaneously, the sequencing results were aligned with the databases (NCBI, dbSNP, HapMap, 1000 human genome datasets, and databases of 100 healthy Chinese adults), and the variants were annotated and screened.

The results of whole-exome sequencing were confirmed using Sanger sequencing, and the sequencing results were aligned with the FBN1 reference sequence (NM_000138.4) to identify mutations.

2.4 | Bioinformatics analysis

Potential pathogenic effects of the variation were evaluated using four algorithms: Mutation Taster (https://www.mutationtaster.org/; Schwarz et al., 2010), Protein Variation Effect Analyzer (PROVEAN, http://provean.jcvi.org/index.php; Choi & Chan, 2015), scale-invariant feature transform (SIFT, http://provean.jcvi.org/index.php; Choi & Chan, 2015), and Polymorphism Phenotyping version2 (PolyPhen-2, http://genetics.bwh.harvard.edu/pph2/; Adzhubei et al., 2010). Damage to the shear site mutation was predicted using the dbNSFP software (http://sites.google.com/site/jpopgen/dbNSFP). The conservation of the mutation site was analyzed using the NCBI BLAST protein blast database.

The Marfan Z-score was calculated based on the patient's sex, height, weight, age, and aortic (Ao) root at the sinuses of Valsalva (http://www.marfan.org).

2.5 | Protein structure analysis

Homology modeling of 3D models of different fragments of fibrillin-1 was created based on the predictions performed using the AlphaFold software (Tunyasuvunakool et al., 2021). The structure and potential consequences of wild-type and mutated fibrillin-1 fragments were displayed using PyMOL 3.1.

2.6 | Protein hydrophobicity and secondary structure analysis

The Kyte-Doolittle algorithm of ProtScale was used to analyze the hydrophobic properties and chemical parameters of the proteins, and the online program GOR4 (https://npsa-prabi.ibcp.fr/cgibin/npsa_automat.pl?page=/NPSA/npsa_gor4.html) was used to analyze the protein secondary structure.

3 | RESULTS

3.1 | Clinical findings

Eight unrelated Chinese families were recruited for the study. All families had congenital lens dislocations and clear family history. The pedigrees and ocular clinical phenotypes of the six isolated EL families are shown in Figure 1, and the pedigrees and clinical phenotypes of the two probands with Marfan syndrome are shown in Figure 2. Detailed examinations were conducted on the ocular, cardiovascular, and skeletal systems of these participants, and the clinical information of all patients in this study was shown in Table 1.

3.2 | Pedigrees 1–6

These six families had a history of congenital lens dislocation and all had bilateral lesions (Figure 1a). The lens dislocation direction was mostly nasal (Figure 1b–g). All 11 participants showed poor binocular vision, and 6 had undergone lens extraction and intraocular lens implantation (Table 1). It is noteworthy that the lens of the left eye of the proband (III: 2) of family 1 had completely prolapsed into the anterior chamber when the patient came to our hospital for treatment, resulting in conjunctival hyperemia and pain (Figure 1b). In family 3, the degree of lens dislocation in the three children

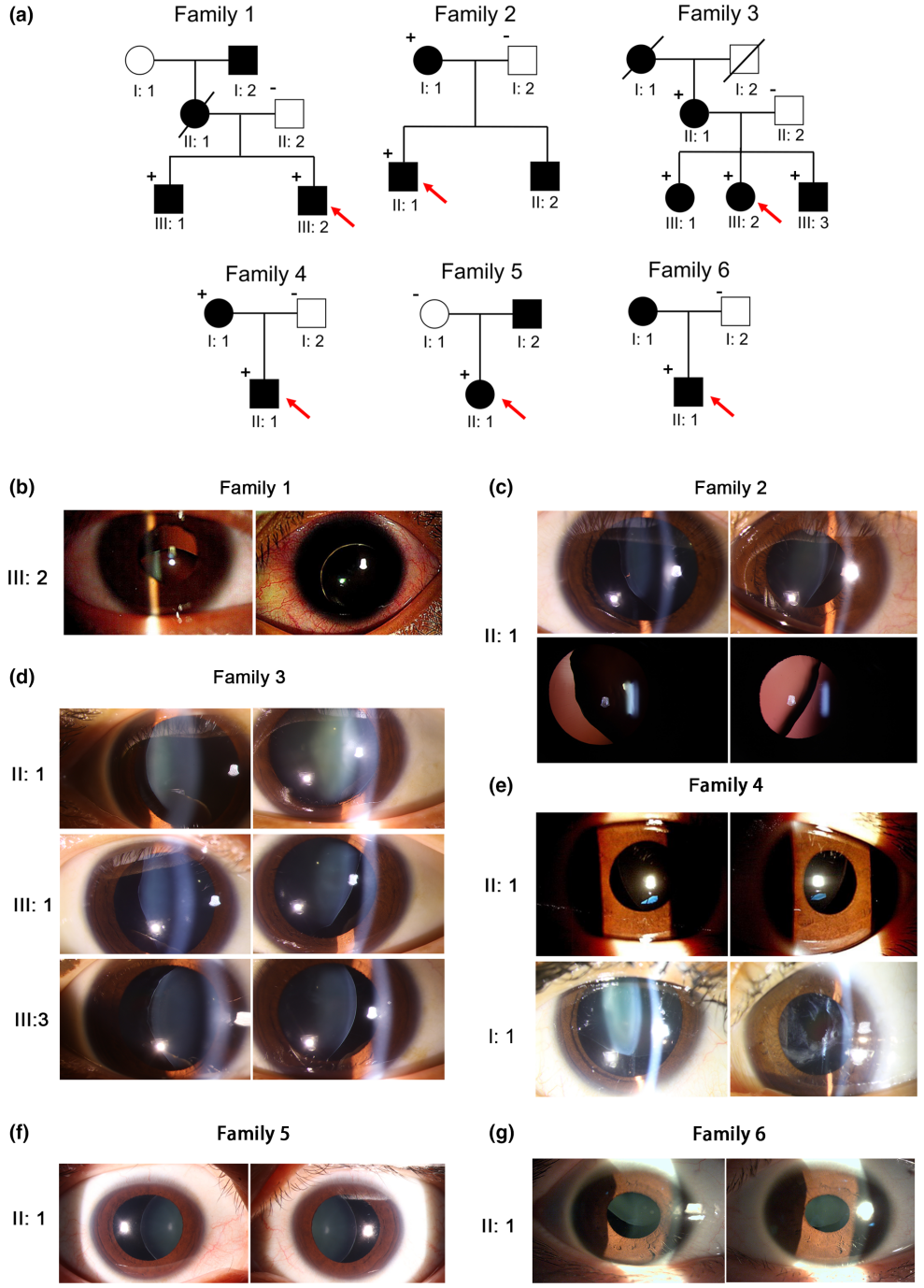

FIGURE 1 Pedigrees and ocular phenotypes of six families with isolated ectopia lentis (EL). (a) Pedigree charts of six families with isolated EL. The dark squares (male) and circles (female) identify the individuals with EL. The red arrow below the patient denotes the proband. Slashes (/) indicate the deceased individuals; +, indicates the individual who carried a heterozygous *FBN1* mutation. −, an individual who does not carry a heterozygous *FBN1* mutation. (b–g) The representative EL phenotype in affected members of families 1–6, respectively. Other family members with EL have similar phenotypes (images not shown).

was relatively severe (representative images in Figure 1d), but the mother's (II: 1 in Figure 1d) left eye had only very slight dislocation. In addition, a slit-lamp examination of the proband of family 4 showed an upward ectopic lens in the right eye and a posterior cataract in the left eye (Figure 1e). No abnormal skeletal or cardiovascular system abnormalities were found in any of the family members.

3.3 | Pedigree 7

Family 7 was a three-generation family with Marfan syndrome and lens dislocation (Figure 2a). The ocular system of the proband was consistent with the characteristics of Marfan syndrome, including lens dislocation and high myopia (Figure 2c). The proband was 179 cm tall and weighed

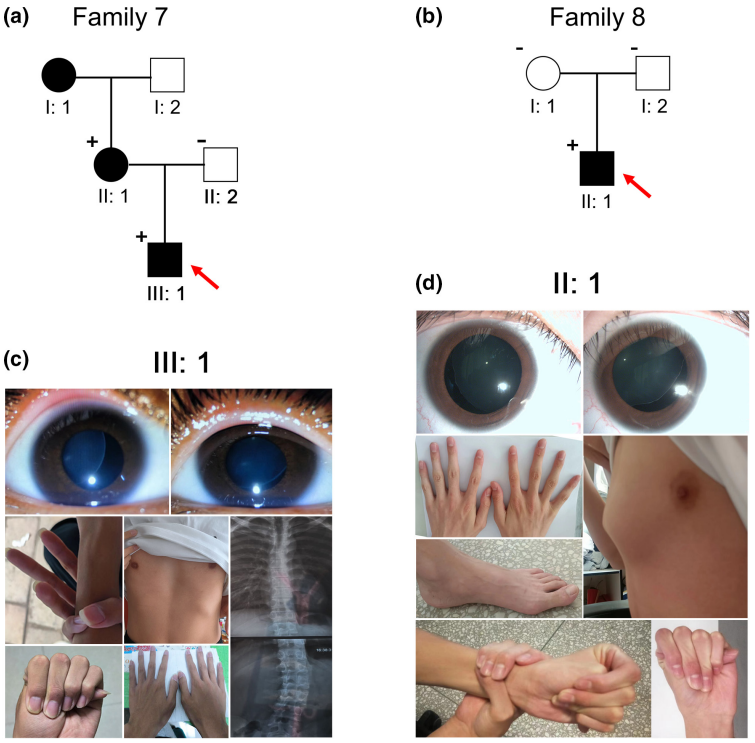

FIGURE 2 Pedigrees and ocular phenotypes of two Marfan syndrome families with ectopia lentis (EL). Pedigree charts of family 7 (a) and family 8 (b). The dark squares (male) and circles (female) indicate the individuals with EL. The red arrow below the patient indicates the proband. +, indicates the individual who carried a heterozygous *FBN1* mutation. −, an individual who does not carry a heterozygous *FBN1* mutation. (c) The proband in family 7 showed bilateral EL, wrist and thumb signs, pectus excavatum, and scoliosis. (d) The proband in family 8 showed bilateral EL, wrist and thumb signs, severe pectus carinatum deformity, and scoliosis.

60 kg and had a positive wrist thumb sign, pectus excavatum, decreased elbow extension, decreased superior/inferior segment ratio, increased arm/height, and scoliosis. Echocardiography of the patient showed no current aortic dilatation (Figure 2c, and Table 1). The patient's maternal grandmother also had lens dislocation and had undergone aortic valve replacement for aortic dilatation. According to the Ghent diagnostic criteria (B. L. Loeys et al., 2010), a proband's systemic score of 8 points can be used to diagnose Marfan syndrome in the presence of family history.

3.4 | Pedigree 8

There was no apparent family history for family 8 (Figure 2b). Patient II: 1 was 16 years old, 183 cm tall, weighed 65 kg, had an AO root at the sinuses of Valsalva of 39 mm, and the calculated Z-score was 2.86. He had lens dislocation in both eyes, high myopia with wrist and thumb signs, severe pectus carinatum deformity, reduced elbow extension, reduced upper segment/lower segment ratio, and increased arm/height; the systemic score was 8 points (Figure 2d, Table 1). According to the Ghent diagnostic criteria (B. L. Loeys et al., 2010), the patient fulfilled the revised Ghent criteria in the absence of a family history of Marfan syndrome.

3.5 | Mutation identification

In eight families with congenital EL, we identified three novel FBN1 mutations, including c.5065G>C (p.D1689H) in II:1, III:1, III:2, and III:3 from family 3, c.1600T>A (p.C534S) in I:1 and II:1 from family 4, and c.2210G>C (p.G737A) in II:1 from family 5, and five previously reported FBN1 mutations including c.364C>T (p.R122C) in III:1 and III:2 from family 1, c.1633C>T (p.R545C) in I:1 and II:1 from family 2, c.718C>T (p.R240C) in II:1 from family 6, c.1543T>C (p.C515R) in II:1 and III:1 from family 7, and c.2687G>A (p.C896Y) in II:1 from family 8 using high-throughput whole-exome and Sanger sequencing (Figure 3a–h, and Table 2). These mutations were located on exons 5–41, of which one was located in the EGF-like domain, four were located in the cbEGF-like domain, one was located in the TB domain, and two were not found in either domain (Table 2). The c.5065G>C mutation was located 1 bp upstream of the spliced region of FBN1. According to our in silico predictions (https://ngdc.cncb.ac.cn/databasecommons/database/id/930), this mutation may affect the splicing process of FBN1, thereby affecting its protein function.

3.6 | Bioinformatics analysis

Protein homology analyses showed that eight mutation sites were highly conserved in fibrillin-1 proteins of different species (Figure 3a–h). All eight mutations were located in exons 5–41, of which four were located in a calcium-binding epidermal growth factor (cbEGF) domain, one was located in an EGF domain, one was located in the TB4 domain, and the other two were

TABLE 1 Clinical characteristics of 13 living patients with congenital ectopia lentis in eight families

Patient	Age (years)	Sex	Diagnosis age (years)	Preoperative BCVA OD/OS	Surgery for EL	Postoperative BCVA	Other
Family 1							
III: 1	32	M	10	FC/30 cm/0.4	Yes	0.4/0.8	—
III: 2	30	M	12	0.5/0.03	Yes	0.7/0.8	—
Family 2							
II: 1	22	M	15	0.1/0.3	No	—	—
Family 3							
II: 1	41	F	37	0.5/0.25	No	—	—
III: 1	19	F	9	0.6/0.5	No	—	—
III: 2	14	F	4	0.2/0.2	Yes	0.5/0.8	—
III: 3	13	M	3	0.3/0.3	No	—	—
Family 4							
II: 1	10	M	6	0.2/0.2	Yes	0.6/0.7	—
I: 1	29	F	3	FC/15 cm/0.3	Yes	0.3/0.7	—
Family 5							
II: 1	27	F	11	0.15/0.2	No	—	—
Family 6							
II: 1	23	M	20	0.25/0.25	Yes	0.6/0.7	—
Family 7							
II: 1	19	M	13	0.2/0.3	Yes	0.7/1.0	Wrist and thumb sign, pectus excavatum, reduced elbow extension, reduced US/LS ratio and increased arm/height, and scoliosis. Systemic score: 8.
Family 8							
II: 1	16	M	9	0.3/0.3	Yes	0.6/0.6	Wrist and thumb sign, severe pectus carinatum deformity, reduced elbow extension, reduced US/LS ratio, and increased arm/height. Systemic score: 8

Abbreviations: BCVA, best corrected visual acuity; EL, ectopia lentis; FC, finger count; OD, oculus dexter; OS, oculus sinister; US/LS, upper segment/lower segment ratio.

not located in a domain of known function (Table 2). The results of MutationTaster, PROVEAN, SIFT, and PolyPhen-2 analyses showed these mutations are deleterious (Table 2).

3.7 | 3D structural analysis of proteins

Compared to the typical protein structure, these missense mutations led to changes in the three-dimensional structure of the FBN1 protein (Figure 4a–h). Among them, three cysteine mutations, C534S, C515R, and C896Y, led to the failure of the formation of disulfide bonds at C534-C546, C515-C528, and C896-C908, respectively (Figure 4d,g,h).

3.8 | Protein hydrophobicity and secondary structure analysis

To explore the effect of these missense mutations on the hydrophobicity and secondary structure of fibrillin-1, we selected different domains, including the mutation site, for analysis. EGF1-EGF3 domains of fibrillin-1 (Fibrillin-$1^{81\text{-}178}$) were used to analyze the consequences of the R122C mutation (Figure 5a); cbEGF7-cbEGF9 domains (Fibrillin-$1^{490\text{-}612}$) were used to analyze the consequences of the R545C, C534S, and C515R mutations (Figure 5b,d,g, respectively); cbEGF28-TB7 domains (Fibrillin-$1^{1648\text{-}1748}$) were used to analyze the consequences of the D1689H mutation (Figure 5c); TB3-cbEGF11 domains

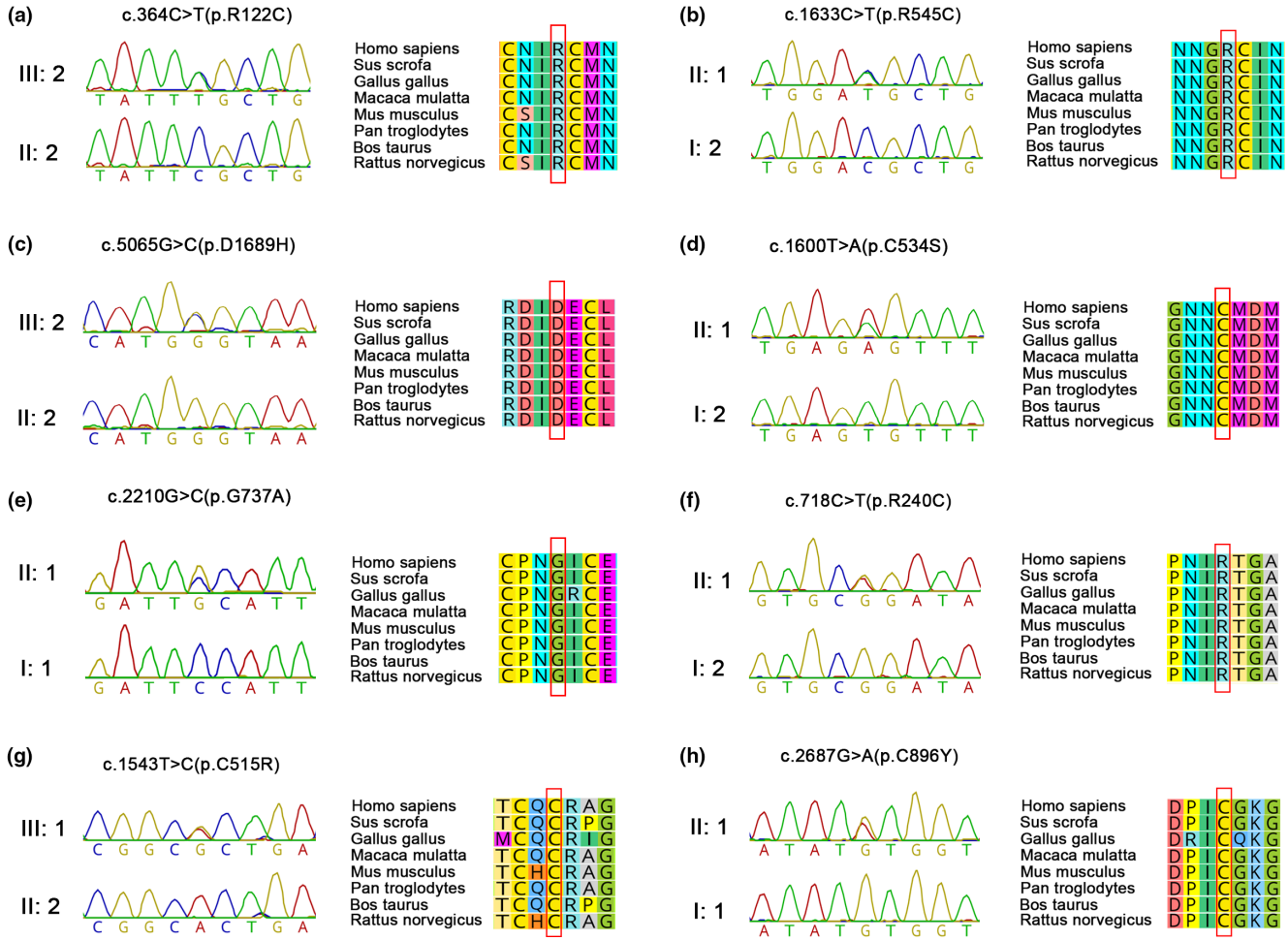

FIGURE 3 Sequence chromatograms and multiple sequence alignments. The *FBN1* variant c.364C>T (p.R122C) is identified in family 1 (A), c.1633C>T (p.R545C) is identified in family 2 (B), c.5065G>C (p.D1689H) is identified in family 3 (C), c.1600T>A (p.C534S) is identified in family 4 (D), c.2210G>C (p.G737A) is identified in family 5 (E), c.718C>T (p.R240C) is identified in family 6 (F), c.1543T>C (p.C515R) is identified in family 7 (G), and c.2687G>A (p.C896Y) is identified in family 8 (H).

(Fibrillin-1$^{659\text{-}764}$) were used to analyze the consequences of the G737A mutation (Figure 5e); TB1-cbEGF4 domains (Fibrillin-1$^{184\text{-}287}$) were used to analyze the consequences of the R240C mutation (Figure 5f); and TB4-cbEGF14 domains of (Fibrillin-1$^{851\text{-}951}$) were used to analyze the consequences of the C896Y mutation (Figure 5h).

Based on ProtScale analysis, most of the eight missense mutations caused significant changes in protein hydrophobicity (Figure 5a–h). Among them, R122C, R545C, G737A, and R240C mutations significantly increased the protein hydrophobicity (Figure 5a,b,e,f). In contrast, C534S, C515R, and C896Y mutations decreased the fibrillin-1 hydrophobicity (Figure 5d,g,h). D1689H mutation led to a slight increase in hydrophobicity (Figure 5c). Molecular prediction by GOR4 showed that all eight missense mutations resulted in significant changes in protein secondary structure, with an abnormal distribution of random structures (Figure 5, highlighted in the green box).

4 | DISCUSSION

Congenital EL is a connective tissue disorder in which the ocular lens is dislocated outside the patellar fossa due to a weakness of the ciliary zonule (Kaur & Gurnani, 2022). Fibrillin-1, coded by the *FBN1* gene, is the main component of microfibrils in the extracellular matrix, and microfibrils are the main components of the lens suspensory ligament (Groth et al., 2017). In addition, microfibers confer fundamental physical and mechanical properties to almost every connective tissue (Baldwin et al., 2013). Mutations in the *FBN1* gene can lead to EL by inhibiting the ciliary zonule function (Groth et al., 2017). Researchers have suggested that EL may not be an independent diagnosis but a mild form of Marfan syndrome (Chandra et al., 2012; Pepe et al., 2007). *FBN1* mutations can lead not only to Marfan syndrome but also Weill–Marchesani syndrome, and other diseases (Schrenk et al., 2018). More than 3000 FBN1 mutations have been identified but only

TABLE 2 The eight *FBN1* variants identified in patients with congenital ectopia lentis

Families	cDNA change	Amino acid change	Exon	Protein domain	SIFT		PolyPhen-2 (HumVar)		PROVEAN		Mutation Taster	Reference
					Score	prediction	Score	prediction	Score	prediction		
Family 1	c.364C>T	R122C	5	EGF-like 2	0.034	DA	0.993	PD	−4.19	DE	DE	Black et al. (1998), Jin et al. (2008), Loeys et al. (2004), Pees et al. (2015), Sthl-Hallengren et al. (1994)
Family 2	c.1633C>T	R545C	14	cb EGF-like 8	0.000	DA	0.998	PD	−7.34	DE	DE	Hayward et al. (1997), Li et al. (2016)
Family 3	c.5065G>C	D1689H	41	-	0.000	DA	0.781	POD	−6.43	DE	DE	This study
Family 4	c.1600T>A	C534S	14	cb EGF-like 8	0.000	DA	0.991	PD	−9.32	DE	DE	This study
Family 5	c.2210G>C	G737A	19	cb EGF-like 11	0.000	DA	0.999	PD	−5.65	DE	DE	This study
Family 6	c.718C>T	R240C	7	-	0.007	DA	0.990	PD	−5.11	DE	DE	Collod-Béroud et al. (1998)
Family 7	c.1543T>C	C515R	13	cb EGF-like 7	0.000	DA	0.996	PD	−11.19	DE	DE	Groth et al. (2017)
Family 8	c.2687G>A	C896Y	23	TB4	0.000	DA	0.997	PD	−9.04	DE	DE	Stheneur et al. (2009)

Abbreviations: cb EGF-like, calcium-binding EGF-like motifs; DA, damaging; DE, deleterious; EGF-like, non-calcium-binding EGF-like motifs; PD, probably damaging; POD, possibly damaging; TO, tolerated.

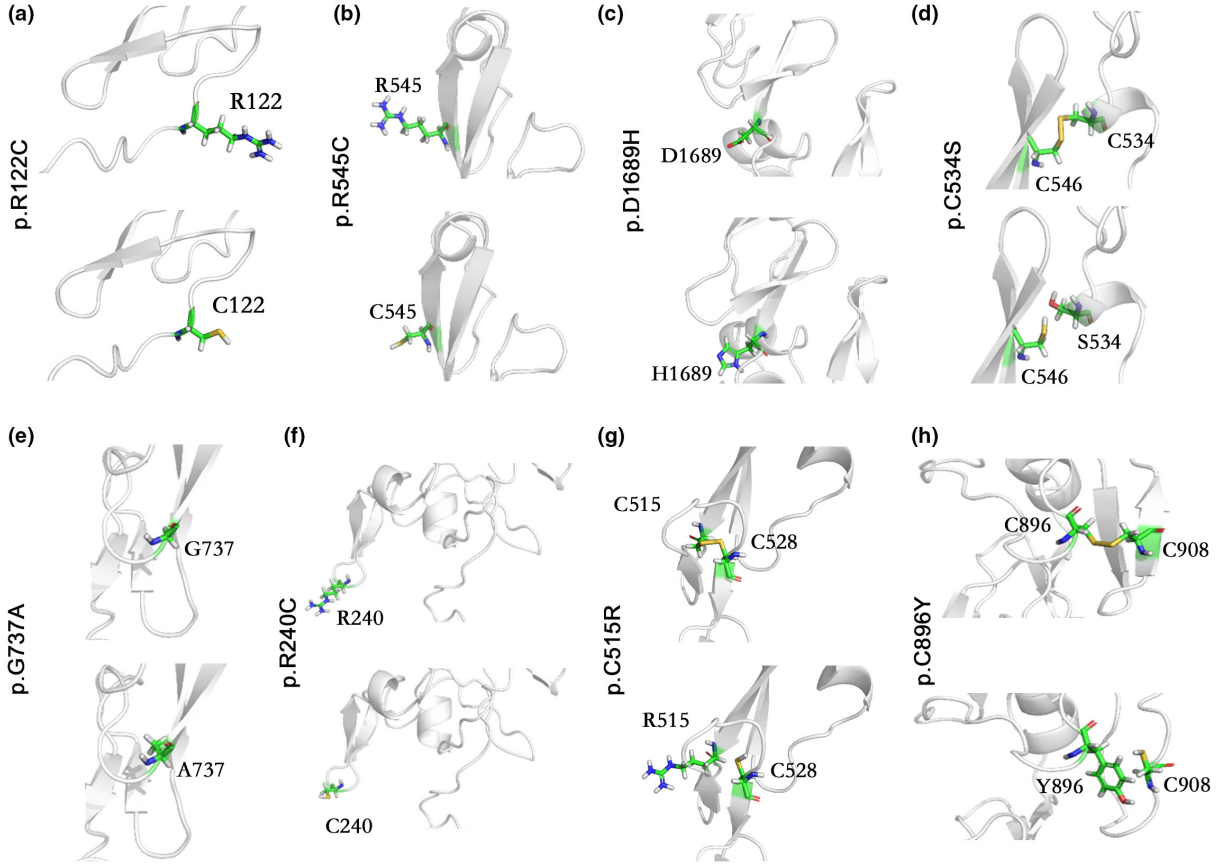

FIGURE 4 Fibrillin-1 protein structure predicted using the AlphaFold software. (A-H) FBN1 mutations that led to the significantly altered 3D structural modeling of the fibrillin-1 polypeptide.

20 have been found in isolated lens dislocations (Yang et al., 2020). In addition, statistics show that only 12% of all reported *FBN1* mutations are recurrent, suggesting that FBN1 mutations are highly heterogeneous between families and many disease-causing mutations remain unknown today (Collod-Béroud et al., 2003). The NGS technologies enable more comprehensive detection of genetic mutations in patients, help diagnose the type of disease, and contributed to the correlation between clinical phenotype and gene mutation analysis. Moreover, this approach allows a definitive genetic diagnosis to identify disease inheritance patterns and avoid genetic defects in offspring.

FBN1 mutations reported to date include substitutions, insertions, deletions, duplications, and other nucleotide changes, which lead to missense, frameshift, nonsense, splice site, and other forms of impact (Stheneur et al., 2009). In this study, eight *FBN1* mutations were, respectively, detected in multiple individuals from six families with isolated EL and two Marfan syndrome families with EL, including c.364C>T (p.R122C) in III:1 and III:2 from family 1; c.1633C>T (p.R545C) in I:1 and II:1 from family 2; c.5065G>C (p.D1689H) in II:1, III:1, III:2, and III:3 from family 3; c.1600T>A (p.534S) in I:1 and II:1 from family 4; and c.2210G>C (p.G737A) in II:1 from family 5; c.718C>T (p.R240C) in II:1 from family 6; c.1543T>C (p.C515R) in II:1 and III:1 from family 7; and c.2687G>A (p.C896Y) in II:1 from family 8. Three of these mutations (i.e., c.5065G>C (p.D1689H), c.1600T>A (p.534S), and c.2210G>C (p.G737A)) were detected and correlated with EL for the first time and the remaining five (i.e., c.364C>T (p.R122C), c.1633C>T (p.R545C), and c.718C>T (p.R240C)) were previously reported. Our results are consistent with previous findings that congenital lens dislocations are most commonly caused by missense mutations in FBN1 (Guo et al., 2021). A previous study has shown that probands with missense mutations tend to exhibit high corneal astigmatism and severe lens dislocation, which is consistent with our current results (Guo et al., 2021). The FBN1 R122C mutation has been previously reported in five families, and they have different clinical phenotypes, but all are accompanied by lens dislocation (Black et al., 1998; Jin et al., 2008; Loeys et al., 2004; Pees et al., 2015; Sthl-Hallengren et al., 1994). Moreover, two patients in a family with this mutation exhibited late-onset cardiovascular disease (Black et al., 1998). Consistent with this, both patients III:1 and III:2 in family 1 suffered EL, but their cardiovascular symptoms

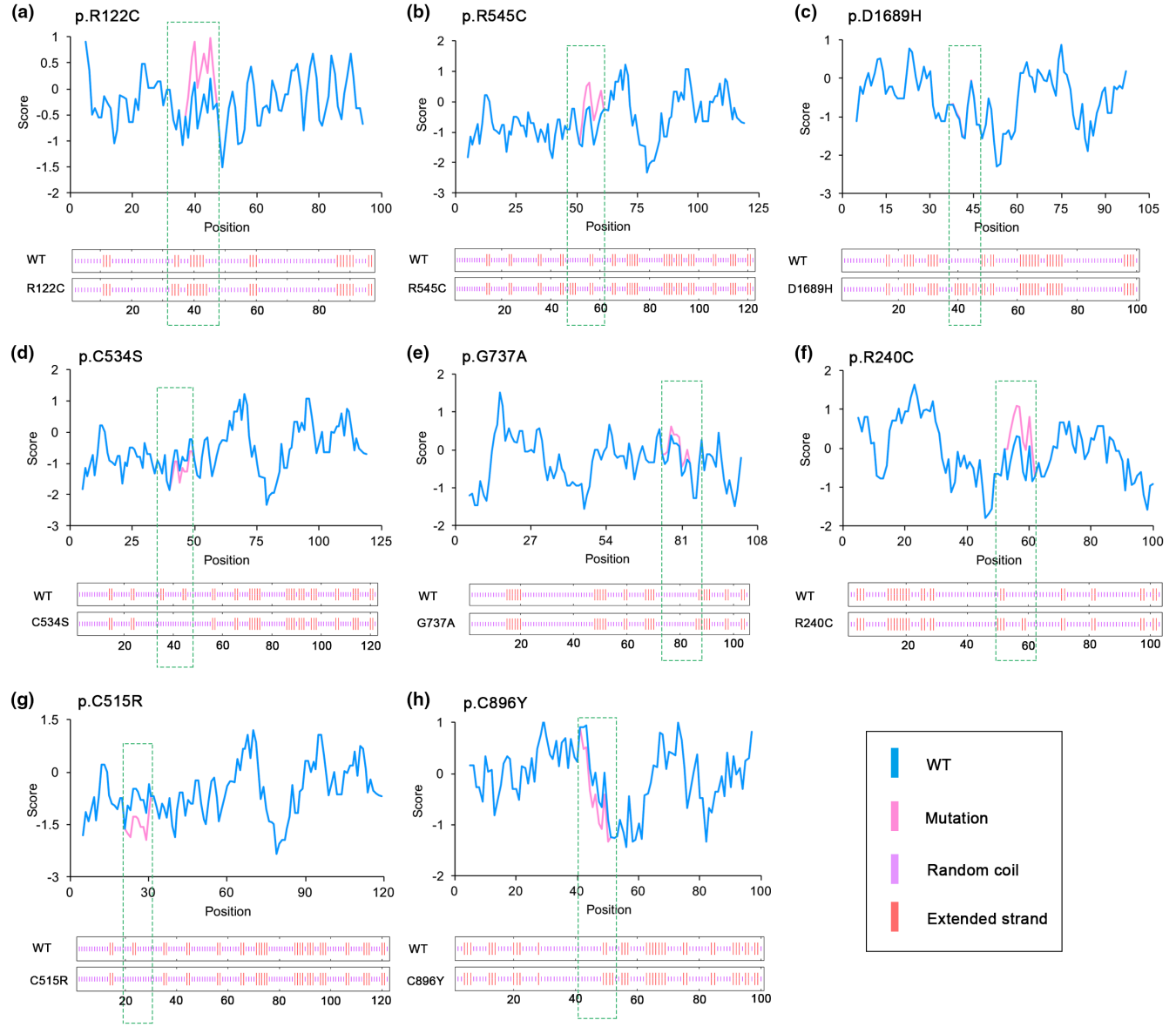

FIGURE 5 Hydrophobicity analysis and secondary structure prediction. (a, b, e, f) The fibrillin-1 R122C, R545C, G737A, and R240C mutations resulted in a significant increase in the hydrophobicity of the surrounding regions and a marked change in the protein secondary structure. (c) The fibrillin-1 D1689H mutation results only in a slight increase in the hydrophobicity of the surrounding region and a marked change in the secondary structure. (d, g, h) The FBN1 C534S, C515R, and C896Y mutations resulted in a slight decrease in the hydrophobicity of its surrounding region and a marked change in the secondary structure.

were not obvious. Since these two patients were young at the time of data acquisition, we cannot exclude the possibility that they might develop additional features of Marfan syndrome in the future, and their cardiovascular symptoms may require follow-up. Both R545C and R240C mutations were reported in a patient with skeletal, ocular, and cardiovascular manifestations; however, only ocular abnormalities were found in patients with these two mutations in our study (Collod-Béroud et al., 1998; Hayward et al., 1997). Furthermore, the R545C mutation was reported in a Chinese family with different Marfan syndrome phenotypes, including EL, aortic dissection, and unaffected individuals (Li et al., 2016). These results indicated that the same FBN1 mutation can lead to a wide range of phenotypes in different countries and even in the same family. It is worth mentioning that the FBN1 mutation G737A identified in family 1 has not been found in patients with EL, but according to the Universal Marfan Database (UMD) predictor tool, this mutation may be pathogenic (Kien et al., 2010).

Unlike isolated lens dislocation with only ocular abnormalities, Marfan syndrome is accompanied by abnormalities of the cardiovascular and skeletal systems, including

pectus carinatum or pectus excavatum deformities, positive wrist and thumb signs, and scoliosis (Loeys et al., 2010). A statistic shows that the incidence of ocular morbidity in patients with Marfan syndrome is approximately 56%, primarily including lens heterotopia, choroid and retinal, refractive, and other abnormalities (Kjeldsen et al., 2022). Here, two recurrent *FBN1* mutations (c.1543T>C (p.C515R) and c.2687G>A (p.C896Y)) were detected in two families with Marfan syndrome and EL. The C515R mutation was also previously reported, but no relevant clinical information is available (Groth et al., 2017). However, the c.1545_1546delinsGG (p.C515W) mutation was detected in patients with Marfan syndrome, EL, and aortic dilatation (Groth et al., 2017). In this study, C515R mutation was detected in a patient with a family history and a clinical phenotype of Marfan syndrome. These results indicate that the cysteine variation at position 515 may be closely related to the occurrence of Marfan syndrome. In addition, the C896Y mutation was detected in the proband of pedigree 8, which is consistent with a mutation detected in a family with a classic Marfan history (Stheneur et al., 2009). The difference is that the proband was the first in his family to show signs and symptoms of Marfan syndrome, including early aortic dilatation, EL, and severe pectus deformity, indicating that this is a sporadic mutation in this individual. This also reminds us that in clinical practice, family history of Marfan syndrome should be assessed but even in the absence of family history, patients with positive signs of Marfan syndrome should undergo genetic testing and regular follow-up with echocardiography. The present findings will support the clinical evaluation of patients with Marfan syndrome by complementing the assessment using this approach.

Consistent with previous reports, the mutations identified in this study (6/8) were primarily located in the 5′ region rather than in the 3′ region or the central portion of the *FBN1*gene (Guo et al., 2021). This may be attributable to the fact that the 5′ region of FBN1 is located at the fibrillin-1 N-terminus and is responsible for the assembly of fibrils and the stability of microfibrils (Meester et al., 2022; Sakai et al., 2016). Fibrillin-1 mainly includes 47 cb or non-cb EGF-like domains, and each EGF-like motif contains six highly conserved cysteine residues that form disulfide bonds in a 1–3, 2–4, and 5–6 arrangement to maintain structural integrity (Downing et al., 1996). Most mutations observed here (5/8) were located in the cbEGF-like or EGF-like domain of fibrillin-1, and five of eight mutations harbored cysteine variation, which is consistent with previous reports that mutations in the EGF-like domain and missense mutations containing cysteine substitutions are common in EL (Rommel et al., 2010; Zhang et al., 2021). Through bioinformatics analysis, we found that the *FBN1* mutation led to obvious changes in the three-dimensional structure, hydrophobicity, and secondary structure of the protein. Three cysteine mutations, C534S, C515R, and C896Y, led to the inability to form disulfide bonds. Cysteine mutations may cause protein misfolding and subsequent dislocation of microfibrils, resulting in abnormal TGF-β signaling (Shi et al., 2011). Moreover, cysteine mutations can affect protein stability, making them more susceptible to protease hydrolysis (Vollbrandt et al., 2004). Patients with cysteine substitutions may have longer axial lengths and poorer preoperative visual acuity (Zhang et al., 2021). In addition, the D1689H mutation was not located within an *FBN1* coding domain but near the splice site and may cause disease by affecting normal *FBN1* splicing.

In summary, we described the clinical manifestations and identified eight *FBN1* mutations in eight Chinese families with congenital EL. Our study had a few limitations. Since most patients were relatively young at the time of this study, the possibility of later concomitant onset of other signs and symptoms cannot be excluded, and further follow-up and observation are needed to verify the clinical manifestations of related mutations. Nevertheless, the results of this study expand the mutation spectrum of congenital EL, helping to clarify the correlation between genotype and phenotype and providing a reference for the early treatment of patients.

AUTHOR CONTRIBUTIONS

XL, JW, and XHL designed and performed the experiments. JW, XHL, and LJ contributed to patient recruitment and clinical data collection. LN and KL analyzed the data. XL, LN, LZ, and XW wrote the manuscript. All authors read and approved the final manuscript.

ACKNOWLEDGMENTS

The authors wish to thank the families for their participation in this study.

FUNDING INFORMATION

This work was supported by the National Nature Science Foundation of China (82070961); the Shenzhen Excellent Technological and Innovative Talent Training Project (RCBS20200714114818372); and the Sanming Project of Medicine in Shenzhen (SZSM201812091).

CONFLICT OF INTEREST

The authors declare that they have no competing interests.

DATA AVAILABILITY STATEMENT

The data that support the finding of this study are available on request from the corresponding author.

ETHICS STATEMENT

This study was performed in accordance with the Declaration of Helsinki and was approved by the

Shenzhen Eye Hospital Ethics Committee (no. 20211 10402).

ORCID

Liman Niu https://orcid.org/0000-0002-9330-4171
Jiantao Wang https://orcid.org/0000-0002-7458-1261

REFERENCES

Adès, L. C., Holman, K. J., Brett, M. S., Edwards, M. J., & Bennetts, B. (2004). Ectopia lentis phenotypes and the FBN1 gene. *American Journal of Medical Genetics. Part A*, *126*(3), 284–289. https://doi.org/10.1002/ajmg.a.20605

Adzhubei, I. A., Schmidt, S., Peshkin, L., Ramensky, V. E., Gerasimova, A., Bork, P., Kondrashov, A. S., & Sunyaev, S. R. (2010). A method and server for predicting damaging missense mutations. *Nature Methods*, *7*(4), 248–249. https://doi.org/10.1038/nmeth0410-248

Al-Salem, M. (1990). Autosomal recessive ectopia lentis in two Arab family pedigrees. *Ophthalmic Paediatrics and Genetics*, *11*(2), 123–127. https://doi.org/10.3109/13816819009012957

Baldwin, A. K., Simpson, A., Steer, R., Cain, S. A., & Kielty, C. M. (2013). Elastic fibres in health and disease. *Expert Reviews in Molecular Medicine*, *15*, e8. https://doi.org/10.1017/erm.2013.9

Black, C., Withers, A. P., Gray, J. R., Bridges, A. B., Craig, A., Baty, D. U., & Boxer, M. (1998). Correlation of a recurrent FBN1 mutation (R122C) with an atypical familial Marfan syndrome phenotype. *Human Mutation*, *Suppl 1*(Supplement S1), S198–S200. https://doi.org/10.1002/humu.1380110164

Chandra, A., Aragon-Martin, J. A., Hughes, K., Gati, S., Reddy, M. A., Deshpande, C., Cormack, G., Child, A. H., Charteris, D. G., & Arno, G. (2012). A genotype-phenotype comparison of ADAMTSL4 and FBN1 in isolated ectopia lentis. *Investigative Ophthalmology & Visual Science*, *53*(8), 4889–4896. https://doi.org/10.1167/iovs.12-9874

Chen, Z., Chen, T., Zhang, M., Chen, J., Deng, M., Zheng, J., Lan, L. N., & Jiang, Y. (2021). Fibrillin-1 gene mutations in a Chinese cohort with congenital ectopia lentis: Spectrum and genotype-phenotype analysis. *The British Journal of Ophthalmology*, *106*, 1655–1661. https://doi.org/10.1136/bjophthalmol-2021-319084

Choi, Y., & Chan, A. P. (2015). PROVEAN web server: A tool to predict the functional effect of amino acid substitutions and indels. *Bioinformatics*, *31*(16), 2745–2747. https://doi.org/10.1093/bioinformatics/btv195

Collod-Béroud, G., Béroud, C., Ades, L., Black, C., Boxer, M., Brock, D. J., Holman, K. J., de Paepe, A., Francke, U., Grau, U., Hayward, C., Klein, H. G., Liu, W., Nuytinck, L., Peltonen, L., Perez, A. B. A., Rantamäki, T., Junien, C., & Boileau, C. (1998). Marfan Database (third edition): New mutations and new routines for the software. *Nucleic Acids Research*, *26*(1), 229–223. https://doi.org/10.1093/nar/26.1.229

Collod-Béroud, G., Le Bourdelles, S., Ades, L., Ala-Kokko, L., Booms, P., Boxer, M., Child, A., Comeglio, P., De Paepe, A., Hyland, J. C., Holman, K., Kaitila, I., Loeys, B., Matyas, G., Nuytinck, L., Peltonen, L., Rantamaki, T., Robinson, P., Steinmann, B., … Boileau, C. (2003). Update of the UMD-FBN1 mutation database and creation of an FBN1 polymorphism database. *Human Mutation*, *22*(3), 199–208. https://doi.org/10.1002/humu.10249

Downing, A. K., Knott, V., Werner, J. M., Cardy, C. M., Campbell, I. D., & Handford, P. A. (1996). Solution structure of a pair of calcium-binding epidermal growth factor-like domains: Implications for the Marfan syndrome and other genetic disorders. *Cell*, *85*(4), 597–605. https://doi.org/10.1016/s0092-8674(00)81259-3

Fuchs, J., & Rosenberg, T. (1998). Congenital ectopia lentis, a Danish national survey. *Acta Ophthalmologica Scandinavica*, *76*(1), 20–26. https://doi.org/10.1034/j.1600-0420.1998.760105.x

Greene, V. B., Stoetzel, C., Pelletier, V., Perdomo-Trujillo, Y., Liebermann, L., Marion, V., De Korvin, H., Boileau, C., Dufier, J. L., & Dollfus, H. (2010). Confirmation of ADAMTSL4 mutations for autosomal recessive isolated bilateral ectopia lentis. *Ophthalmic Genetics*, *31*(1), 47–51. https://doi.org/10.3109/13816810903567604

Groth, K. A., Von Kodolitsch, Y., Kutsche, K., Gaustadnes, M., Thorsen, K., Andersen, N. H., & Gravholt, C. H. (2017). Evaluating the quality of Marfan genotype-phenotype correlations in existing FBN1 databases. *Genetics in Medicine*, *19*(7), 772–777. https://doi.org/10.1038/gim.2016.181

Guo, D., Jin, G., Zhou, Y., Zhang, X., Cao, Q., Lian, Z., Guo, Y., & Zheng, D. (2021). Mutation spectrum and genotype-phenotype correlations in Chinese congenital ectopia lentis patients. *Experimental Eye Research*, *207*, 108570. https://doi.org/10.1016/j.exer.2021.108570

Haller, S. J., Roitberg, A. E., & Dudley, A. T. (2020). Steered molecular dynamic simulations reveal Marfan syndrome mutations disrupt fibrillin-1 cbEGF domain mechanosensitive calcium binding. *Scientific Reports*, *10*(1), 16844. https://doi.org/10.1038/s41598-020-73969-2

Hayward, C., Porteous, M. E., & Brock, D. J. (1997). Mutation screening of all 65 exons of the fibrillin-1 gene in 60 patients with Marfan syndrome: Report of 12 novel mutations. *Human Mutation*, *10*(4), 280–289. https://doi.org/10.1002/(sici)1098-1004(1997)10:4<280::aid-humu3>3.0.co;2-l

Hoffman, R. S., Snyder, M. E., Devgan, U., Allen, Q. B., Yeoh, R., & Braga-Mele, R. (2013). Management of the subluxated crystalline lens. *Journal of Cataract & Refractive Surgery*, *39*(12), 1904–1915. https://doi.org/10.1016/j.jcrs.2013.09.005

Jin, C., Yao, K., Sun, Z., & Wu, R. (2008). Correlation of the recurrent FBN1 mutation (c.364C>T) with a unique phenotype in a Chinese patient with Marfan syndrome. *Japanese Journal of Ophthalmology*, *52*(6), 497–499. https://doi.org/10.1007/s10384-008-0586-y

Kaur, K., & Gurnani, B. (2022). Ectopia Lentis. In *StatPearls*. StatPearls Publishing. https://www.ncbi.nlm.nih.gov/books/NBK578193/

Kien, P., Baux, D., Pallares-Ruiz, N., Baudoin, C., Plancke, A., Chassaing, N., Collignon, P., Drouin-Garraud, V., Hovnanian, A., Martin-Coignard, D., & Collod-Béroud, G. (2010). Missense mutations of conserved glycine residues in fibrillin-1 highlight a potential subtype of cb-EGF-like domains. *Human Mutation*, *31*(1), E1021–E1042. https://doi.org/10.1002/humu.21131

Kjeldsen, S., Andersen, N., Groth, K., Larsen, D., Hjortdal, J., Berglund, A., Gravholt, C., & Stochholm, K. (2022). Ocular morbidity in Marfan syndrome: A nationwide epidemiological study. *The British Journal of Ophthalmology*. https://doi.org/10.1136/bjophthalmol-2021-320871

Li, Y., Xu, J., Chen, M., Du, B., Li, Q., Xing, Q., & Zhang, Y. (2016). A FBN1 mutation association with different phenotypes of

Marfan syndrome in a Chinese family. *Clinica Chimica Acta*, *460*, 102–106. https://doi.org/10.1016/j.cca.2016.06.031

Loeys, B., Backer, J. D., Acker, P. V., Wettinck, K., Pals, G., Nuytinck, L., Coucke, P., & Paepe, A. D. (2004). Comprehensive molecular screening of the FBN1 gene favors locus homogeneity of classical Marfan syndrome. *Human Mutation*, *24*(2), 140–146. https://doi.org/10.1002/humu.20070

Loeys, B. L., Dietz, H. C., Braverman, A. C., Callewaert, B. L., De Backer, J., Devereux, R. B., Hilhorst-Hofstee, Y., Jondeau, G., Faivre, L., Milewicz, D. M., Pyeritz, R. E., Sponseller, P. D., Wordsworth, P., & De Paepe, A. M. (2010). The revised Ghent nosology for the Marfan syndrome. *Journal of Medical Genetics*, *47*(7), 476–485. https://doi.org/10.1136/jmg.2009.072785

Lygia, P., Marina, D., Francesco, R., Jennifer, R. L., Bryan, S., Theresa, P., & Jeffrey, B. (1993). Genomic organization of the sequence coding for fibrillin, the defective gene product in Marfan syndrome. *Human Molecular Genetics*, *2*(7), 961–968. https://doi.org/10.1093/hmg/2.10.1762

Meester, J. A. N., Peeters, S., Van Den Heuvel, L., Vandeweyer, G., Fransen, E., Cappella, E., Dietz, H. C., Forbus, G., Gelb, B. D., Goldmuntz, E., Hoskoppal, A., Landstrom, A. P., Lee, T., Mital, S., Morris, S., Olson, A. K., Renard, M., Roden, D. M., Singh, M. N., … Loeys, B. L. (2022). Molecular characterization and investigation of the role of genetic variation in phenotypic variability and response to treatment in a large pediatric Marfan syndrome cohort. *Genetics in Medicine*, *24*, 1045–1053. https://doi.org/10.1016/j.gim.2021.12.015

Milewicz, D. M., Braverman, A. C., De Backer, J., Morris, S. A., Boileau, C., Maumenee, I. H., Jondeau, G., Evangelista, A., & Pyeritz, R. E. (2021). Marfan syndrome. *Nature Reviews Disease Primers*, *7*(1), 64. https://doi.org/10.1038/s41572-021-00298-7

Nelson, L. B., & Maumenee, I. H. (1982). Ectopia lentis. *Survey of Ophthalmology*, *27*(3), 143–160. https://doi.org/10.1016/0039-6257(82)90069-8

Pees, C., Michel-Behnke, I., Hagl, M., & Laccone, F. (2015). Detection of 15 novel mutations in 52 children from 40 families with the Marfan or Loeys–Dietz syndrome and phenotype–genotype correlations. *Clinical Genetics*, *86*(6), 552–557. https://doi.org/10.1111/cge.12314

Pepe, G., Lapini, I., Evangelisti, L., Attanasio, M., Giusti, B., Lucarini, L., Fattori, R., Pellicanò, G., Scrivanti, M., Porciani, M. C., Abbate, R., & Gensini, G. F. (2007). Is ectopia lentis in some cases a mild phenotypic expression of Marfan syndrome? Need for a long-term follow-up. *Molecular Vision*, *13*, 2242–2247. https://doi.org/10.1186/1471-2199-8-108

Rommel, K., Karck, M., Haverich, A., Kodolitsch, Y. V., & Arslan-Kirchner, M. (2010). Identification of 29 novel and nine recurrent fibrillin-1 (FBN1) mutations and genotype-phenotype correlations in 76 patients with Marfan syndrome. *Human Mutation*, *26*(6), 529–539. https://doi.org/10.1002/humu.20239

Sadiq, M. A., & Vanderveen, D. (2013). Genetics of ectopia Lentis. *Seminars in Ophthalmology*, *28*(5–6), 313–320. https://doi.org/10.3109/08820538.2013.825276

Sakai, L. Y., & Keene, D. R. (2019). Fibrillin protein pleiotropy: Acromelic dysplasias. *Matrix Biology*, *80*, 6–13. https://doi.org/10.1016/j.matbio.2018.09.005

Sakai, L. Y., Keene, D. R., Renard, M., & De Backer, J. (2016). FBN1: The disease-causing gene for Marfan syndrome and other genetic disorders. *Gene*, *591*(1), 279–291. https://doi.org/10.1016/j.gene.2016.07.033

Schrenk, S., Cenzi, C., Bertalot, T., Conconi, M. T., & Di Liddo, R. (2018). Structural and functional failure of fibrillin-1 in human diseases (review). *International Journal of Molecular Medicine*, *41*(3), 1213–1223. https://doi.org/10.3892/ijmm.2017.3343

Schwarz, J. M., Rödelsperger, C., Schuelke, M., & Seelow, D. (2010). MutationTaster evaluates disease-causing potential of sequence alterations. *Nature Methods*, *7*(8), 575–576. https://doi.org/10.1038/nmeth0810-575

Shi, M., Zhu, J., Wang, R., Chen, X., Mi, L., Walz, T., & Springer, T. A. (2011). Latent TGF-β structure and activation. *Nature*, *474*(7351), 343–349. https://doi.org/10.1038/nature10152

Stheneur, C., Collod-Beroud, G., Faivre, L., Buyck, J. F., Gouya, L., Le Parc, J. M., Moura, B., Muti, C., Grandchamp, B., Sultan, G., Claustres, M., Aegerter, P., Chevallier, B., Jondeau, G., & Boileau, C. (2009). Identification of the minimal combination of clinical features in probands for efficient mutation detection in the FBN1 gene. *European Journal of Human Genetics*, *17*(9), 1121–1128. https://doi.org/10.1038/ejhg.2009.36

Sthl-Hallengren, C., Ukkonen, T., Kainulainen, K., Kristofersson, U., & Peltonen, L. (1994). An extra cysteine in one of the non-calcium-binding epidermal growth factor-like motifs of the FBN1 polypeptide is connected to a novel variant of Marfan syndrome. *Journal of Clinical Investigation*, *94*(2), 709–713. https://doi.org/10.1172/JCI117389

Tunyasuvunakool, K., Adler, J., Wu, Z., Green, T., Zielinski, M., Žídek, A., Bridgland, A., Cowie, A., Meyer, C., Laydon, A., Velankar, S., Kleywegt, G. J., Bateman, A., Evans, R., Pritzel, A., Figurnov, M., Ronneberger, O., Bates, R., Kohl, S. A. A., … Hassabis, D. (2021). Highly accurate protein structure prediction for the human proteome. *Nature*, *596*(7873), 590–596. https://doi.org/10.1038/s41586-021-03828-1

Vollbrandt, T., Tiedemann, K., El-Hallous, E., Lin, G., Brinckmann, J., John, H., Bätge, B., Notbohm, H., & Reinhardt, D. P. (2004). Consequences of cysteine mutations in calcium-binding epidermal growth factor modules of fibrillin-1. *The Journal of Biological Chemistry*, *279*(31), 32924–32931. https://doi.org/10.1074/jbc.M405239200

Yang, Y., Zhou, Y. L., Yao, T. T., Pan, H., & Wang, Z. Y. (2020). Novel p.G1344E mutation in FBN1 is associated with ectopia lentis. *British Journal of Ophthalmology*, *105*, 341–347. https://doi.org/10.1136/bjophthalmol-2019-315265

Zeyer, K. A., & Reinhardt, D. P. (2015). Engineered mutations in fibrillin-1 leading to Marfan syndrome act at the protein, cellular and organismal levels. *Mutation Research/Reviews in Mutation Research*, *765*, 7–18. https://doi.org/10.1016/j.mrrev.2015.04.002

Zhang, M., Chen, Z., Chen, T., Sun, X., & Jiang, Y. (2021). Cysteine substitution and calcium-binding mutations in FBN1 cbEGF-like domains are associated with severe ocular involvement in patients with congenital ectopia lentis. *Frontiers in Cell and Development Biology*, *9*, 816397. https://doi.org/10.3389/fcell.2021.816397

How to cite this article: Liu, X., Niu, L., Zhang, L., Jiang, L., Liu, K., Wu, X., Liu, X., & Wang, J. (2023). Clinical and genetic findings in Chinese families with congenital ectopia lentis. *Molecular Genetics & Genomic Medicine*, *11*, e2140. https://doi.org/10.1002/mgg3.2140